

Temperature and Viscosity Dependence of the Triplet Energy Transfer Process in Porphyrin Dimers

Joakim Andréasson^a, Alexander Kyrychenko^{a,b}, Jerker Mårtensson^c,
and Bo Albinsson^{*a}

^aDepartment of Physical Chemistry and ^cDepartment of Organic Chemistry
Chalmers University of Technology, SE-412 96
Göteborg, Sweden

^bPermanent address: Research Institute for Chemistry, Kharkov State University,
4, Svobody Sq., 310077 Kharkov, Ukraine

Correspondence to: Bo Albinsson, Department of Physical Chemistry, Chalmers
University of Technology, SE-412 96 Göteborg, Sweden

Phone: 46-31-772 30 44

Fax: 46-31-772 38 58

e-mail: balb@phc.chalmers.se

Submitted to PPS (Photochemical and Photobiological Sciences) 010829

Abstract

The temperature and viscosity dependence of the triplet energy transfer (TET) process in porphyrin dimers have been studied. A zinc porphyrin (donor) and a free base porphyrin (acceptor) are covalently linked together by rigid bridging chromophores at a center-center distance of 25 Å. Due to the large donor-acceptor distance and the weakness of the spin forbidden transitions involved, neither Dexter nor Förster mechanisms are expected to contribute to the observed TET process. The results from transient absorption measurements at temperatures between room temperature and 80 K show that TET occurs with unexpected high efficiency in the systems connected with fully conjugated bridges and a pronounced temperature dependence of the process is observed. Comparison of the TET efficiencies in dimers connected by different bridging chromophores correlates well with a transfer reaction governed by the superexchange mechanism. However, in high viscosity media the TET process is dramatically slowed down. This is attributed to a conformational gating of the TET process where the electronic coupling varies strongly with the relative orientation of the donor and the bridging chromophore. Further, the zinc porphyrin donor offers two distinct donor species, T_{1A} and T_{1B} . At room temperature, the TET rate constant of the T_{1A} species is about two orders of magnitude larger than for the T_{1B} species. The dimers studied are well suited model systems for materials where the rate of the transfer reactions can be changed by external stimuli.

Introduction

The transfer of electrons and excitation energy between porphyrins in supramolecular systems is an area under intensive investigation.¹⁻⁷ The relevance of these processes in Nature is obvious when describing the reactions that constitute the photosynthetic apparatus. Light harvesting by the chlorophylls triggers the chain of events that, via consecutive steps of energy and electron transfer, ends up with charge separation in the reaction center. Several model systems have been designed in order to mimic the natural photosynthesis.⁸⁻¹⁴ A lot of effort has also been made to get insight into the mechanisms and the set of parameters (structural, photophysical etc.) that determines the efficiency of the processes mentioned above.¹⁵⁻¹⁷ Particular attention has been given to the factors that are believed to influence the magnitude of the essential electronic coupling that governs the transfer reactions. One of these factors is the electronic structure of the intervening medium between the donor and the acceptor. The most common way to separate the donor from the acceptor is to link them by a third molecule. Where the Nature uses a protein matrix, chemists most often use covalent bonds and rigid spacers to get a well-defined molecular architecture and to ensure the building-blocks, Donor-Bridge-Acceptor (D-B-A), to be electronically isolated. The study of intramolecular transfer reactions in D-B-A systems offers some clear advantages compared to intermolecular transfer between diffusing species separated by solvent molecules. The rigidity of the systems makes it possible to isolate the crucial D-A distance and the functional

similarities between the bridges and the protein framework found in biological systems makes them better candidates for the mimicry of natural photosynthesis. The D-B-A systems also provides the possibility to investigate the superexchange mechanism, suggested some 40 years ago in which the bridge contributes in the transfer reaction by propagating the electronic interaction between donor and acceptor.¹⁸⁻²⁰

One of the factors that is expected to influence the magnitude of the electronic coupling is the energy splitting between the lowest excited states of the bridge and the donor. In recent works, we showed that in a series of porphyrin dimers linked together by different bridging chromophores, the rates of singlet and triplet energy transfer increases as the energy of the lowest singlet and triplet excited state of the bridge successively approaches the energy of the donor excited state.²¹⁻²³ In this work we have extended the studies to include the temperature and viscosity dependence of the triplet energy transfer (TET) process. It was shown in reference 21 that TET in compound ZnP-OB-H₂P (Figure 1) where the conjugation in the bridge is broken was dramatically slower compared to the compounds ZnP-BB-H₂P and ZnP-NB-H₂P with fully conjugated bridges. We have, in fact, not been able to detect any TET at all in the ZnP-OB-H₂P dimer why this paper focuses on the ZnP-BB-H₂P and ZnP-NB-H₂P dimers.

Another interesting feature is the conformational flexibility and various non-planar distortions of the porphyrin macrocycle induced by a sterically

encumbered substitution pattern.²⁴⁻²⁹ Recently, we showed that the intrinsic relaxation of the lowest electronically excited triplet state of both the donor and the acceptor porphyrin subunits, in the dimers studied, actually involves two different “mother-daughter” related species each, arbitrarily called T_{1A} and T_{1B} .³⁰ It was also shown that the transformation process $T_{1A} \rightarrow T_{1B}$ most likely is accompanied by conformational changes. Part of this work has focused on comparing the properties of the T_{1A} and T_{1B} species of the zinc porphyrin donor with respect to the triplet energy transfer properties. In rigid media, such as in an organic glass or a polymer matrix, the transformation into the T_{1B} species is expected to be hindered. In order to simplify the analysis and to concentrate on the TET process that emanates from the T_{1A} species, a series of measurements at high viscosity was performed. This also turned out to yield new information on the medium effect and the dynamical nature of the TET process. The TET seems to be gated by thermal excitations in the bonds connecting the bridge and donor chromophores which gives a pronounced viscosity dependence.

Experimental Section

Materials. The synthesis and purification of the reference compounds (ZnP-BB and ZnP-NB) and the dimers (ZnP-BB-H₂P and ZnP-NB-H₂P) are described elsewhere.³¹ The structures of all studied compounds are shown in Figure 1. The spectroscopic measurements were performed with either 2-methyltetrahydrofuran (MTHF, purchased from ACROS), a 1:6 mixture of

toluene/methylcyclohexan (toluene/MCH, purchased from LAB-SCAN and MERCK, respectively), a 1:1 mixture of toluene/polystyrene (toluene/PS), or polystyrene- (PS) films as the solvent. The PS-films were prepared by adding the porphyrinic compounds, dissolved in toluene, into a hot 10% (w/w) solution of PS in toluene. The crude PS-pellets (average M.W.= 250.000) were purchased from ACROS. The mixtures were stirred for two hours to form optically clear solutions. The films were prepared by gently pouring the hot solutions onto glass plates. After two days of drying under controlled vapor pressure, the porphyrin concentration of the films were approximately $1-5 \times 10^{-4}$ M. Before measurements, the films were mounted into a cryostat and vacuum pumped for 12 hours to remove oxygen and solvent residues.

Spectroscopic Measurements. Ground state absorption spectra were recorded using a CARY 4B UV/Vis spectrometer. Triplet lifetimes were determined by laser flash photolysis or by xenon lamp pulsed excitation followed by time resolved gated phosphorescence detection using a SPEX 1934D3 phosphorimeter. In the flash photolysis experiments the excitation source was the 532 nm second harmonics of a Nd/YAG laser (Spectron Laser Systems SL803G1270). The monitoring system consisted of a pulsed xenon lamp followed by a conventional monochromator photomultiplier system (symmetrical Czerny-Turner arrangement and a 5 stage Hamamatsu R928). Data acquisition was performed via a Philips model PM 3323 digital oscilloscope. In order to minimize interference from triplet annihilation and self-quenching and to avoid

kinetic distortions caused by inhomogeneities in the sample distribution, the ground state absorption at 532 nm was adjusted to 0.05 and the T_1 - T_n absorption was kept below 0.15.³² In the temperature interval in which transient absorption was measured, the triplet lifetimes of the compounds studied showed no concentration dependence. This excludes that bimolecular processes limit the triplet lifetimes. Ground state absorption spectra recorded after the transient absorption measurements showed neither significant bleaching nor additional absorption bands. The kinetic traces were formed by averaging between 16 and 64 recorded decay curves. A minimum of six kinetic traces at different wavelengths were then analyzed by global analysis methodology. All samples were carefully degassed by six freeze-pump-thaw cycles to a final pressure of ca. 10^{-4} torr. Low temperature measurements were done in a nitrogen cooled cryostat (Oxford Instruments) equipped with a temperature regulator. The triplet excitation energies of the different species were estimated from the 0-0 phosphorescence transitions measured at 80 K or from comparison with similar molecules.

Results

The primary objectives of this work have been to investigate the effect of temperature and solvent viscosity on the rate of intramolecular triplet energy transfer. The result section is organized as follows: First, we describe the design criteria applied to the dimers and the intrinsic photophysical properties of the

porphyrin reference compounds. Second, results from the series of measurements at different temperatures in a non-viscous solvent (MTHF) are presented. Finally, the influence of the solvent viscosity is investigated by performing similar measurements in three solutions with vastly different viscosities (toluene/MCH, toluene/PS, and PS-film) in the temperature interval between 295 and 80 K.

In the following sections the experimental results (Figures) will be shown only for one of the dimers, ZnP-NB-H₂P, and the corresponding reference compounds, ZnP-NB and H₂P-NB in one of the solvents (MTHF). The evaluated data of all compound and solvent combinations studied will be collected in the Tables.

General Considerations. *Design.* The dimers investigated in this paper consist of a zinc porphyrin (ZnP, energy donor) and a free base porphyrin (H₂P, energy acceptor) at 25 Å center-center distance (see Figure 1). The porphyrins are covalently linked together by either of three different bridging chromophores. The primary objectives in designing the dimers shown in Figure 1 was to achieve a system that promoted detailed studies on how the electronic structure of the bridges influences the energy transfer process. It is, therefore, very important to minimize the variation of other structural and photophysical parameters in the dimers that are known to affect the rate of energy transfer. The different design criteria are thoroughly discussed in reference 22. Briefly, the center-center distance between donor and acceptor in all the dimers are estimated to 25.3 Å based on molecular mechanics (MM+) ³³ calculations. The relative orientation of

the donor and the acceptor is also independent of the bridging chromophore, and simple π -conjugation between the subunits is minimized in order to keep the donor, bridge, and acceptor electronically isolated.

Properties of the Porphyrin Reference Compounds. As mentioned in the Introduction, the triplet excited state relaxation of the zinc and free base porphyrin reference compounds involves two “mother-daughter” related species. The various processes participating in the overall deactivation of zinc porphyrin in a D-B-A system are discussed in reference 30 and summarized in Figure 2. Intersystem crossing from the excited singlet state populates the mother species, or the T_{1A} species. At high temperatures (165 K and above) the T_{1A} species is efficiently deactivated (≈ 100 ns at room temperature) via a transformation process to the T_{1B} species. Due to the substantial activation energy of the transformation process, (about 7 kcal/mol) it is virtually shut off at lower temperatures, and the deactivation is governed by direct intersystem crossing, $T_{1A} \rightarrow S_0$. The T_{1B} species relaxation, $T_{1B} \rightarrow S_0$, is also unusually efficient yielding μ s lifetime of the porphyrin triplet species (T_{1B}) at room temperature. It is also worth noticing that in a highly viscous media, the transformation process is not observed, and the T_{1A} species is deactivated exclusively by direct intersystem crossing to the ground state at all temperatures. The triplet lifetimes in these high viscosity media are in the ms regime which is in accordance with other non-sterically encumbered porphyrins such as octaalkyl- or tetraphenylporphyrins. The lifetime data of the donor moieties, i.e. the ZnP-RB reference compounds, in

MTHF, toluene/MCH, toluene/PS, and PS-films are comprised in Tables 1, 2, 3, and 4, respectively.

Triplet Excitation Energies. The energy diagram of the lowest excited triplet states of the donor, bridge and acceptor subunits are shown in Figure 3.³⁴ On energetic grounds, it is seen that TET from ZnP to H₂P is possible. The different electronic structures of the bridging chromophores are reflected in the energies of the lowest triplet states and increases in the order NB, BB, and OB. To be able to attribute differences regarding the rates of TET to a pure mediation effect of the bridges, it is crucial to exclude stepwise energy transfer, Donor → Bridge → Acceptor. The smallest energy splitting between donor and bridge in the dimers studied here is 3 500 cm⁻¹ (NB), which is one order of magnitude larger than the average thermal energy at room temperature. Therefore, it is not very likely that the stepwise route makes a large contribution to the overall rate of TET.

Room Temperature Ground State and T₁-T_n Absorption Spectra. The ground state and the T₁-T_n absorption spectra ($\lambda_{\text{exc}}=532$ nm) of ZnP-NB and H₂P-NB in MTHF are shown in Figures 4 and 5, respectively. At 532 nm, the ratio $\epsilon_{532}(\text{ZnP})/\epsilon_{532}(\text{H}_2\text{P})$ is about 3 why the ZnP chromophore is accounted for 75 % of the absorbed excitation light in the dimers. Based on the results from previous studies on the same systems, where the efficiencies of singlet energy transfer at room temperature was found to be 0.40, and 0.44 for ZnP-BB-H₂P and ZnP-NB-H₂P, respectively,²³ in combination with literature data on the quantum

yield of intersystem crossing,³⁵ the yield of triplet formation would be approximately 0.40 for ZnP and 0.45 for H₂P in the dimers (upon excitation at 532 nm). This provides a situation well suited for probing the deactivation of the donor and acceptor excited triplet states.

Decay Kinetics of the Dimers. TET from ZnP to H₂P in the dimers is an additional deactivation channel from the triplet excited species of ZnP (cf. Figure 2). Therefore, comparing the triplet lifetime of ZnP in the dimers, τ , and the reference compounds, τ_0 , will give the rate constant of TET, k_{TET} , from eq. (1).

$$k_{\text{TET}} = 1/\tau - 1/\tau_0 \quad (1)$$

As is seen in Figure 5, there is no wavelength to probe exclusively the decay of the ZnP triplet. Therefore, the transient absorption decays from the dimers must be analyzed by resolving the contributions from both the ZnP and H₂P subunits. As the relaxation of ZnP and H₂P excited states in non-viscous solutions at room temperature involve two triplet species each, there are in total four different lifetimes to resolve in each transient. However, at most temperatures this problem can be avoided. Given that the lifetimes are different enough, altering the range of the probing light time window simplifies the fitting procedure to include a maximum of three exponentials in each time window. First we have characterized the TET properties of the T_{1A} species by using a short time window. Later the corresponding T_{1B} species measurements are performed with a longer time window.

Decay Kinetics in MTHF. *Room Temperature, 295 K.* In an attempt to determine the rate of TET from ZnP T_{1A} species in the ZnP-BB-H₂P and ZnP-NB-H₂P dimers at room temperature, the shortest time window possible was used to probe the decay. A fast decay in the early part of the transients was observed, with a lifetime of approximately 50 ns. However, the instrumental time resolution is not optimal in this range, and, in addition, the H₂P T_{1A} species decay is expected to contribute to the overall transient absorption profile with a similar lifetime (140 ns in the H₂P-NB reference compound). Therefore, at room temperature, we do not draw any quantitative conclusions about the TET rate from the ZnP T_{1A} species. In the longer time window measurements, bi-exponential analysis of the T_{1B} species transient decays resulted in the ZnP lifetimes shown in Table 1. The significantly decreased triplet lifetime of ZnP in the ZnP-BB-H₂P and ZnP-NB-H₂P dimers clearly shows that TET makes a significant contribution to the T_{1B} species overall deactivation process in these dimers. The corresponding rate constants, k_{TETB} , are collected in Table 1. The equivalent energy transfer efficiencies, calculated as

$$E_{TETB} = 1 - \tau_B / \tau_{0B} \quad (2)$$

would then be 0.21 and 0.31 for the ZnP-BB-H₂P and ZnP-NB-H₂P dimers, respectively.

Low temperatures, 250-120 K. The temperature effect on the intramolecular quenching of ZnP triplet state in the dimers is expected to reveal some valuable information about the mechanism of TET. Therefore, transient

absorption measurements were used to quantify the rate of TET down to 120 K. The transients from ZnP-NB-H₂P recorded at 250 K, using both a short and a long time window, illustrates well the different relaxation routes of ZnP and H₂P in the dimers. In the short time window, (Figure 6, Inset) the lifetime of the ZnP T_{1A} species is readily determined from the fast decay in the early part of the transient, $\tau = 95$ ns. As the corresponding lifetime of the H₂P subunit is expected to be about 1.3 μ s (from the H₂P-NB reference compound), interference from this decay to the 95 ns lifetime should be negligible. Comparing the lifetime of the ZnP T_{1A} species in the ZnP-NB reference compound (470 ns) and in the ZnP-NB-H₂P dimer (95 ns), the rate constant of TET from the T_{1A} species, k_{TETA} , would be $8.4 \times 10^6 \text{ s}^{-1}$. It is worth pointing out that the relevant transition of the H₂P acceptor moiety involved in this TET process most likely is S₀→T_{1A} as we showed in reference 30 that the T_{1B} species can only be populated via the T_{1A}→T_{1B} transformation process. As $k_{\text{TETA}} = 8.4 \times 10^6 \text{ s}^{-1}$ corresponds to a TET efficiency of 80 %, the transformation process T_{1A}→T_{1B} should populate the ZnP T_{1B} species with 20 % efficiency. Therefore, we would expect three distinct processes to be reflected in the long time window (Figure 6):

- 1) Transformation, T_{1A}→T_{1B}, of the H₂P subunit.
- 2) Intersystem crossing, T_{1B}→S₀, of the H₂P subunit.
- 3) Intersystem crossing, T_{1B}→S₀, of the ZnP subunit.

Indeed, the transient could not be properly analyzed by including less than three exponentials in the fitting procedure.

$$\Delta A_{\text{tot}}(t) = \alpha_1 \exp(-t/\tau_1) + \alpha_2 \exp(-t/\tau_2) + \alpha_3 \exp(-t/\tau_3) \quad (3)$$

The best fit to eq. (3) was obtained with the following lifetimes and preexponential factors: $\tau_1 = 6.3 \mu\text{s}$, $\alpha_1 = 0.013$; $\tau_2 = 12.5 \mu\text{s}$, $\alpha_2 = 0.039$; and $\tau_3 = 1.7 \mu\text{s}$, $\alpha_3 = -0.011$. Comparing the lifetimes in the dimer and the corresponding reference compounds ZnP-NB (6.7 μs) and H₂P-NB (1.3 and 12.2 μs for the transformation and the intersystem crossing process, respectively) at 250 K, the processes 1-3 mentioned above could be identified. As the 1.7 and 12.5 μs lifetimes are ascribed to the H₂P subunit, they are combined in Figure 6 to show the overall time evolution of the H₂P absorption in the long time window. The decay profile of ZnP T_{1B} species absorption is also shown ($\tau = 6.3 \mu\text{s}$). Because three similar lifetimes are resolved from the same transient and taking into account the uncertainties impaired by the fitting procedure, the quenching efficiency of the ZnP T_{1B} species in the dimers is not evaluated.

At 200 K the short time window measurements resulted in the lifetimes shown in Table 1. As inferred from the high quenching efficiencies of the ZnP T_{1A} species in the ZnP-NB-H₂P and ZnP-BB-H₂P dimers, 99 and 95 %, respectively, the transformation process T_{1A}→T_{1B} makes only a minor contribution to the overall deactivation. Hence, the T_{1B} species population of ZnP in the dimers is expected to be small. This is confirmed from the long time window measurements, where only the decay characteristics of the H₂P moieties could be resolved. At temperatures of 150 K and lower, the rate of TET is at least three orders of magnitude larger than the other deactivation channels (T_{1A}→T_{1B}

transformation and $T_{1A} \rightarrow S_0$ intersystem crossing) why the T_{1A} species of ZnP in the dimers is exclusively deactivated by TET. Furthermore, the measurements at 150 K established that the decay of ZnP T_{1A} species is paralleled by the building up of the corresponding H_2P triplet as a risetime is seen in the transient probed at 434 nm where the triplet absorption from H_2P dominates (not shown).

Decay Kinetics in Solvents of Different Viscosity. The temperature dependence of the triplet decay kinetics in the dimers and the reference compounds was studied in three additional solvents/media. The solvent mixtures or media used were, in order of increasing viscosity, toluene/MCH (1:6), toluene/PS (1:1), and PS-film. The experimental details and the analysis of the data were the same as in the series of measurements in MTHF, although a broader temperature interval was covered here (RT-80 K). As a result of this, the glass-setting temperatures of the two solvent mixtures are passed in decreasing the temperature, giving rise to a dramatic change in the viscosity. In the PS-film, though, there is no such phase-transition temperature, why the viscosity changes with temperature are much less pronounced. It is also worth noticing that only the lifetime of the T_{1A} species can be resolved from the measurements in PS-film at all temperatures. Again, this is due to the high viscosity of the PS-film, which efficiently inhibits the transformation process $T_{1A} \rightarrow T_{1B}$. The lifetime data of ZnP in the reference compounds and the dimers are collected in Tables 2-4.

Discussion.

Mechanism of the Triplet Energy Transfer Process. In general, energy transfer reactions are described in terms of either Förster (dipole-dipole interaction)^{36, 37} or Dexter (exchange interaction)³⁸ mechanisms. The Förster theory is usually applied to describe long-range energy transfer whereas the Dexter theory is used when the transitions relevant for the energy transfer process are forbidden or very weak. A prerequisite though for the Dexter mechanism to be operative is that the donor and acceptor orbitals overlap. Therefore, for the Dexter mechanism to make significant contribution to the overall energy transfer process, the donor and acceptor should be at contact distance. In the dimers studied in this work, the center-center distance between donor and acceptor is 25 Å. The direct orbital overlap is therefore negligible, why the Dexter mechanism is not expected to contribute significantly. Considering the very weak nature of the spin forbidden singlet to triplet and triplet to singlet transitions involved in the energy transfer process, the Förster mechanism is clearly ruled out. The lifetimes of the compounds studied showed no dependence on concentration, why intermolecular processes also can be excluded. Stepwise energy transfer from donor via bridge to acceptor is excluded for energetic reasons. Therefore, it is most likely that the electronic coupling is mediated by the bridge virtual states, i.e. that the superexchange mechanism dominates the triplet energy transfer reaction. Given that the electronic coupling

between the donor and acceptor is described by the weak coupling case, the Fermi golden rule should be applicable to predict the rate constant of TET,

$$k_{\text{TET}} = (4\pi^2/h)|V|^2(\text{FCWD}) \quad (4)$$

where $|V|$ is the electronic coupling element and (FCWD) is the Franck-Condon weighed density of states. Since it has been shown that long range triplet energy transfer can be regarded as concerted hole and electron transfer from the donor to the acceptor moiety,^{39, 40} the same set of parameters used to describe a non-adiabatic electron transfer reaction can be employed here:

$$k_{\text{TET}} = v \cdot \exp(-\Delta G^\ddagger/RT) \quad (5)$$

$$v = \frac{2|V|^2}{h} (\pi^3 / \lambda RT)^{1/2} \quad (6)$$

$$\Delta G^\ddagger = \frac{\lambda}{4} (1 + \Delta G^0 / \lambda)^2 \quad (7)$$

where λ is the total reorganization energy and ΔG^0 is the free energy change of the TET process. Combining eqs. (5) and (6) allows us to estimate the activation energy, ΔG^\ddagger , from the slope of the straight line

$$\ln(k_{\text{TET}} \cdot \sqrt{T}) = \ln \left(\frac{2|V|^2}{h} (\pi^3 / \lambda R)^{1/2} \right) - \frac{\Delta G^\ddagger}{RT} \quad (8)$$

Figure 7 shows the plots $\ln(k_{\text{TET}} \cdot T^{1/2})$ vs. $1/T$ for ZnP-BB-H₂P and ZnP-NB-H₂P in fluid MTHF (i.e. above 120 K). The free energies of activation are found to be 1.0 and 1.1 kcal/mol, respectively. The electronic coupling element, $|V|$, can be determined from the intercept if the reorganization energy, λ , is known. Since the

temperature interval covered by the series of measurements spans the range between room temperature and 120 K, λ is not expected to be constant. However, it has been argued that the internal vibrational reorganization energy, λ_v , dominates the reorganization energy for energy transfer⁴¹⁻⁴⁴ and we assume, to a first approximation, that it is temperature independent. Triplet energy transfer does not involve large charge redistribution and the solvent (outer) reorganization energy should therefore be much smaller than observed for electron transfer reactions.

As the temperature dependence of λ is not expected to be large, it is disregarded to facilitate the determination of ΔG^\ddagger and $|V|$. The driving force for triplet energy transfer, ΔG^0 , is estimated from the triplet energies of the donor and acceptor. The T_{1A} species of ZnP is phosphorescent and from the 0-0 transition the energy is estimated to be 14000 cm^{-1} .³⁴ We have not been able to detect any phosphorescence from the acceptor (H_2P) but literature values for free base porphyrins places their lowest triplet energies in the range $11500 - 13000 \text{ cm}^{-1}$.³⁵ In fact, Zenkevich and co-workers observed phosphorescence from a structurally similar free base porphyrin with a triplet energy of 12400 cm^{-1} .⁴⁵ Using this value gives an estimate for the driving force to -1600 cm^{-1} , which yields $\lambda = 0.50 \text{ eV}$ (4000 cm^{-1}). From the intercepts in Figure 7, $|V| = 0.18 \text{ cm}^{-1}$ and 0.43 cm^{-1} are derived for ZnP-BB- H_2P and ZnP-NB- H_2P , respectively. As the coupling between donor and acceptor in the dimers studied is expected to be

dominated by the superexchange mechanism, the electronic coupling element should be proportional to the inverse energy difference between the donor and bridge excited states, ΔE_{DB} .¹⁸ From phosphorescence measurements (not shown) the energy differences between the ZnP donor moiety and the two bridging chromophores, BB and NB, are 6000 and 3500 cm^{-1} , respectively. Therefore, the superexchange mechanism predicts the coupling element to increase by a factor 1.7 in going from ZnP-BB-H₂P to ZnP-NB-H₂P, which is to be compared with the observed value of 2.3.

The temperature dependence for the TET process in the solvents which undergo large viscosity changes shows a different behavior. Figure 8 shows a modified Arrhenius plots for these measurements in toluene/MCH, toluene/PS and PS. At temperatures above the glass-setting temperatures a significant temperature dependence is observed along with electronic couplings of similar magnitudes as was observed for MTHF. In contrast, at temperatures below the glass-setting temperatures (i.e. at all temperature for PS) much smaller temperature dependencies and electronic couplings are observed. The estimated numerical values for the free energy of activation, reorganization energies, and electronic couplings are collected in Tables 5 and 6 for the NB and BB bridged systems, respectively. A few things need to be commented on. It is encouraging that the reorganization energies and activation energies, which are properties associated with the donor and acceptor, does not depend on the bridging chromophore. The reorganization energies does not depend strongly on the

solvent polarity but are significantly reduced in solid state. This is expected since the reorganization energies are dominated by internal properties of the donor and acceptor rather than on the solvent properties (*vide supra*). The electronic coupling, on the other hand, is significantly different for the ZnP-BB-H₂P and ZnP-NB-H₂P systems. This is also expected since the bridge plays an instrumental role in mediating the electronic coupling, and, as was argued in an earlier section, the coupling seems to reflect the behavior of the superexchange model.

The electronic coupling is dramatically reduced in the solid solutions. For the PS dissolved dimers this reduction is easily detected in the much slower TET rates at room temperature. The reason for this large difference is not definitely established, but we believe that the increased conformational flexibility in the triplet manifold, compared to the ground state, is important for gating the electronic coupling.³⁰ We have calculated the electronic coupling quantum mechanically for electron transfer and studied its dependence on the bridge conformations for similar systems.⁴⁶ The electronic coupling depends strongly on the dihedral angle between the porphyrin macrocycle and the first phenyl plane (Figure 1) yielding a significant temperature dependence of the electronic coupling. A simplified model where the electronic coupling is given by the π - π overlap between the donor and bridge chromophores would predict that

$$V(\phi) = V_0 \cos \phi \quad (9)$$

where ϕ is the dihedral angle and V_0 is the electronic coupling for coplanar

phenyl and porphyrin planes. Since the angle ϕ is temperature dependent due to the Boltzmann distribution of conformations and the minimum in the ground state lies at $\phi = 90^\circ$ where the coupling is zero, the electronic coupling is expected to increase with temperature giving the rate of TET a non-Arrhenius behavior. In the above analysis the electronic coupling was assumed to be temperature independent, although having different values above and below the glass-transition temperature. Even though the fits in Figures 7 and 8 seem reasonable there is certainly room for improvement. A simple test where the electronic coupling was allowed to increase linearly with temperature did not significantly change the quality of the fit and it is not possible from only the data in fluid solution to judge whether the electronic coupling should be allowed to vary with temperature or not. We know, however, that the porphyrins used in this study undergo conformational changes in the triplet manifold, most likely accompanied by twisting the phenyl substituents.^{30, 45} Consequently, the ground state Boltzmann distribution of the D-B-A systems with ϕ near 90° and, thus, low electronic coupling is changed in the triplet state to a situation where the phenyl groups could rotate towards the plane of the porphyrin macrocycle generating substantially larger electronic coupling. When the solvent rigidifies this conformational freedom is lost and the donor can not adopt a conformation where its coupling to the bridge is as large, thus, explaining the much slower TET in solid media. Wasielewski, Ratner and Davis recently discussed a similar conformational gating for electron transfer reactions in oligo-p-

phenylvinylenes.⁴⁷ Further evidence for conformational-dependent electronic coupling might be seen from the experiments in a highly viscous region near the glass-setting temperatures of the solvents. At these conditions, the expected monoexponential donor decay becomes more complex and can not be resolved into less than two components with the additional long-lived lifetime accounting for approximately 10-15% of the decay. Such a kinetic behavior is most probably due to slow interconversion between rotational conformers, occurring at the time scale of TET. A similar behavior was also observed for the oligo-p-phenylvinylenes, when linked to a donor in a structurally similar way as in our systems.⁴⁷

It is clearly important to further study these intriguing exceptions from the simple Marcus /Hush⁴⁸⁻⁵² and Jortner⁵³ theories in which the electronic coupling is regarded to be a constant, and we plan to further develop systems to address these questions directly.

Another interesting feature observed regarding the TET process in the dimers is the difference in reactivity towards energy transfer for the two distinct donor species of ZnP, i.e. the T_{1A} and T_{1B} species. At room temperature, the difference between k_{TETA} and k_{TETB} is estimated to be about two orders of magnitude. This difference is most likely a result of lowering the energy of the donor excited triplet state in going from the T_{1A} to the T_{1B} species. As a natural consequence, the driving force for the reaction is decreased. This provides a situation of “one donor chromophore-two donor species”. Please note that in our

model for the TET from the T_{1A} species the donor increases its electronic coupling to the bridge because the porphyrin is more conformationally flexible in the triplet manifold compared to the ground state. The same conformational flexibility allows the molecule to pass into the second minimum (T_{1B}) with lower energy and driving force for TET. This conformational gating of TET might have interesting applications in biological and artificial systems as the rate of energy transfer can be altered by imposing conformational constraints on the molecular subunits involved in the transfer reaction.

Conclusions

The temperature and viscosity dependence of the triplet energy transfer (TET) process in covalently linked porphyrin dimers has been investigated. From this study the following has been learned:

- 1) The fully conjugated bridging chromophores (BB and NB) mediate long-range TET between the porphyrin donor and acceptor. In a bridge where the π -conjugation is broken (OB) no long-range TET was observed.
- 2) The TET process is strongly temperature dependent with free energies of activation in the range 1-1.7 kcal/mol in low viscosity solvents. In high viscosity solvents the temperature dependence is much less pronounced.
- 3) The electronic coupling for TET is about 2 times larger for the NB-bridged system compared to the BB-bridged system in good agreement with expectations from the superexchange model.
- 4) In high viscosity medium the rate of TET slows down dramatically due to much smaller electronic coupling. It is argued that the triplet excited donor porphyrin can adopt conformations in fluid solution which has a much larger electronic coupling than what is possible for the same molecule in high viscosity media. This implies a temperature and viscosity dependent electronic coupling, yielding expected deviations from established theories for electron and energy transfer.

5) In solvents of low viscosity at sufficiently high temperatures the donor passes into a second triplet species, T_{1B} . TET occurs also from this species but with about 100 times slower rates presumably due to lower driving force.

Acknowledgement

This work was supported by grants from the Swedish Natural Science Research Council (NFR) and the Swedish Research Council for Engineering Science (TFR).

References and Notes

- 1 O. Ohno, Y. Ogasawara, M. Asano, Y. Kajii, Y. Kaizu, K. Obi, and H. Kobayashi, *J. Phys. Chem.*, 1987, **91**, 4269-4273.
- 2 A. Harriman, V. Heitz, and J.-P. Sauvage, *J. Phys. Chem.*, 1993, **97**, 5940-5946.
- 3 M. Asano-Someda and Y. Kaizu, *Inorg. Chem.*, 1999, **38**, 2303-2311.
- 4 L. Flamigni, F. Barigelletti, N. Armaroli, B. Ventura, J.-P. Collin, J.-P. Sauvage, and J. A. G. Williams, *Inorg. Chem.*, 1999, **38**, 661-667.
- 5 A. M. Brun, A. Harriman, V. Heitz, and J.-P. Sauvage, *J. Am. Chem. Soc.*, 1991, **113**, 8657-8663.
- 6 A. Harriman, V. Heitz, M. Ebersole, and H. van Willigen, *J. Phys. Chem.*, 1994, **98**, 4982-4989.
- 7 H. Levanon, A. Regev, and P. K. Das, *J. Phys. Chem.*, 1987, **91**, 14-16.
- 8 H. Kurreck and M. Huber, *Angew. Chem. Int. Ed. Engl.*, 1995, **34**, 849-866.
- 9 J. Krasnovsky, A. A., M. E. Bashtanov, N. N. Drozdova, P. A. Liddell, A. L. Moore, T. A. Moore, and D. Gust, *Photochem. Photobiol. A*, 1997, **102**, 157-161.
- 10 D. Gust, T. A. Moore, A. L. Moore, D. Kuciauskas, P. A. Liddell, and B. D. Halbert, *Photochem. Photobiol. B*, 1998, **43**, 209-216.

- 11 A. Osuka, H. Yamada, K. Maruyama, N. Mataga, T. Asahi, M. Ohkouchi, T. Okada, I. Yamazaki, and Y. Nishimura, *J. Am. Chem. Soc.*, 1993, **115**, 9439-9452.
- 12 M. Freemantle, *Chem. Eng. News*, 1998, 37-46.
- 13 D. Kuciauskas, P. A. Lidell, S. Lin, T. E. Johnson, S. J. Weghorn, J. S. Lindsey, A. L. Moore, T. A. Moore, and D. Gust, *J. Am. Chem. Soc.*, 1999, **121**, 8604-8614.
- 14 L. Sun, L. Hammarström, B. Åkermark, and S. Styring, *Chem. Soc. Rev.*, 2001, **30**, 36-49.
- 15 S. Speiser, *Chem. Rev.*, 1996, **96**, 1953-1976.
- 16 J.-P. Sauvage, J.-P. Collin, J.-C. Chambron, S. Guillerez, C. Coudret, V. Balzani, F. Barigilletti, L. De Cola, and L. Flamigni, *Chem. Rev.*, 1994, **94**, 993-1019.
- 17 J.-C. Chambron, A. Harriman, V. Heitz, and J.-P. Sauvage, *J. Am. Chem. Soc.*, 1993, **115**, 7419-7425.
- 18 H. M. McConnell, *J. Chem. Phys.*, 1961, **35**, 508-515.
- 19 J. Halpern and L. E. Orgel, *Discuss. Faraday Soc.*, 1960, **29**, 32-41.
- 20 P. W. Anderson, *Phys. Rev.*, 1950, **79**, 350-356.
- 21 J. Andréasson, J. Kajanus, J. Mårtensson, and B. Albinsson, *J. Am. Chem. Soc.*, 2000, **122**, 9844-9845.

- 22 K. Kilså, J. Kajanus, J. Mårtensson, and B. Albinsson, *J. Phys. Chem. B.*, 1999, **103**, 7329-7339.
- 23 K. K. Jensen, S. B. van Berlekom, J. Kajanus, J. Mårtensson, and B. Albinsson, *J. Phys. Chem. A*, 1997, **101**, 2218-2220.
- 24 K. M. Barkigia, M. D. Berber, J. Fajer, C. J. Medforth, M. W. Renner, and K. M. Smith, *J. Am. Chem. Soc.*, 1990, **112**, 8851-8857.
- 25 S. Gentemann, C. J. Medforth, T. P. Forsyth, D. J. Nurco, K. M. Smith, J. Fajer, and D. Holten, *J. Am. Chem. Soc.*, 1994, **116**, 7363-7368.
- 26 M. W. Renner, R.-J. Cheng, C. K. Chang, and J. Fajer, *J. Phys. Chem.*, 1990, **94**, 8508-8511.
- 27 L. D. Sparks, C. J. Medforth, M.-S. Park, J. R. Chamberlain, M. R. Ondrias, M. O. Senge, K. M. Smith, and J. A. Shelnut, *J. Am. Chem. Soc.*, 1993, **115**, 581-592.
- 28 C. M. Drain, C. Kirmaier, C. J. Medforth, D. J. Nurco, K. M. Smith, and D. Holten, *J. Phys. Chem.*, 1996, **100**, 11984-11993.
- 29 M. Ravikanth, and T. K. Chandrashekar. In *Structure and Bonding*, Vol. 82; Springer-Verlag: Berlin Heidelberg, 1995; p 105-188.
- 30 J. Andréasson, H. Zetterqvist, J. Kajanus, J. Mårtensson, and B. Albinsson, *J. Phys. Chem. A*, 2000, **104**, 9307-9314.
- 31 J. Kajanus, S. B. van Berlekom, B. Albinsson, and J. Mårtensson, *Synthesis*, 1999, 1155-1162.

- 32 R. Bonneau, J. Wirz, and A. D. Zuberbühler, *Pure Appl. Chem.*, 1997, **69**,
979-992.
- 33 The MM+ force field as implemented in the program package
HyperChem 5.1, Hypercube Inc.
- 34 The T_{1A} species is the lowest phosphorescent state of the porphyrins
studied. Most likely, the T_{1B} species is lower in energy, but as it is non-
phosphorescent at all temperatures where it is populated, the energy has
not been determined.
- 35 S. L. Murov, and I. Carmichael. *Handbook of Photochemistry*, 2nd ed.;
Marcel Dekker: New York, 1993.
- 36 T. Förster, *Naturwiss.*, 1946, **33**, 166-175.
- 37 T. Förster, *Ann. Physik*, 1948, **2**, 55-75.
- 38 D. L. Dexter, *J. Chem. Phys.*, 1953, **21**, 836-850.
- 39 G. L. Closs, P. Piotrowiak, J. M. MacInnis, and G. R. Fleming, *J. Am.*
Chem. Soc., 1988, **110**, 2652-2653.
- 40 G. L. Closs, M. D. Johnson, J. R. Miller, and P. Piotrowiak, *J. Am. Chem.*
Soc., 1989, **111**, 3751-3753.
- 41 I. Place, A. Farran, K. Deshayes, and P. Piotrowiak, *J. Am. Chem. Soc.*,
1998, **120**, 12626-12633.
- 42 M. A. Sigman and G. L. Closs, *J. Phys. Chem.*, 1991, **95**, 5012-5017.

- 43 D. B. MacQueen, J. R. Eyler, and K. S. Schanze, *J. Am. Chem. Soc.*, 1992, **114**, 1897-1898.
- 44 Z. Murtaza, D. K. Graff, A. P. Zipp, L. A. Worl, W. E. Jones, W. D. Bates, and T. J. Meyer, *J. Phys. Chem.*, 1994, **98**, 10504-10513.
- 45 V. Knyukshto, E. Zenkevich, E. Sagun, A. Shulga, and S. Bachilo, *Chem. Phys. Lett.*, 1998, **297**, 97-108.
- 46 K. Kilså, J. Kajanus, S. Larsson, A. N. Macpherson, J. Mårtensson, and B. Albinsson, *Chem. Eur. J.*, 2001, **7**, 2122-2133.
- 47 W. B. Davis, M. A. Ratner, and M. R. Wasielewski, *J. Am. Chem. Soc.*, 2001, **123**, 7877-7886.
- 48 R. A. Marcus, *J. Chem. Phys.*, 1956, **24**, 966-978.
- 49 R. A. Marcus, *Annu. Rev. Phys. Chem.*, 1964, **15**, 155-196.
- 50 R. A. Marcus and N. Sutin, *Biochim. Biophys. Acta*, 1985, **811**, 265-322.
- 51 N. S. Hush, *Trans. Faraday Soc.*, 1961, **57**, 577-580.
- 52 N. S. Hush, *J. Chem. Phys.*, 1958, **28**, 962-972.
- 53 J. Jortner, *J. Chem. Phys.*, 1976, **64**, 4860-4867.

TABLE 1: Triplet Lifetimes of ZnP in MTHF at Different Temperatures and the Corresponding Rate Constants for Triplet Energy**Transfer.**

	ZnP-NB			ZnP-NB-H ₂ P			ZnP-BB			ZnP-BB-H ₂ P		
	$\tau_A/\mu\text{s}$	$\tau_B/\mu\text{s}$	$\tau_A/\mu\text{s}$	$\tau_B/\mu\text{s}$	$k_{\text{TETA}}/\text{s}^{-1}$	$k_{\text{TETB}}/\text{s}^{-1}$	$\tau_A/\mu\text{s}$	$\tau_B/\mu\text{s}$	$\tau_A/\mu\text{s}$	$\tau_B/\mu\text{s}$	$k_{\text{TETA}}/\text{s}^{-1}$	$k_{\text{TETB}}/\text{s}^{-1}$
295 K	0.073	5.4	-	3.7	-	8.5×10^4	0.086	5.1	-	4.1	-	4.8×10^4
250 K	0.47	6.7	0.095	-	8.4×10^6	-	0.60	6.5	0.27	-	2.0×10^6	-
200 K	16	8.4	0.20	-	4.9×10^6	-	16	8.5	0.91	-	1.0×10^6	-
150 K	2400	a	0.28	-	3.6×10^6	-	2600	a	1.38	-	7.2×10^5	-
120 K	34000	a	0.98	-	1.0×10^6	-	32000	a	3.6	-	2.8×10^5	-

^a At temperatures of 150 K and lower, the kinetics of the T_{IB} species can not be properly resolved because the depopulation is much faster than the formation, and therefore shows too vague traces in the transients.

TABLE 2: Triplet Lifetimes of ZnP in Toluene/MCH (1:6) at Different Temperatures and the Corresponding Rate Constants for Triplet**Energy Transfer.**

	ZnP-NB			ZnP-NB-H ₂ P			ZnP-BB			ZnP-BB-H ₂ P		
	$\tau_A/\mu\text{s}$	$\tau_B/\mu\text{s}$	$\tau_A/\mu\text{s}$	$\tau_B/\mu\text{s}$	$k_{\text{TETA}}/\text{s}^{-1}$	$k_{\text{TETB}}/\text{s}^{-1}$	$\tau_A/\mu\text{s}$	$\tau_B/\mu\text{s}$	$\tau_A/\mu\text{s}$	$\tau_B/\mu\text{s}$	$k_{\text{TETA}}/\text{s}^{-1}$	$k_{\text{TETB}}/\text{s}^{-1}$
295 K	0.15	5.7	-	4.1	-	6.8×10^4	0.17	6.0	-	4.7	-	4.4×10^4
250 K	1.4	7.6	0.08	-	1.2×10^7	-	1.5	7.9	0.25	-	3.3×10^6	-
225 K	3.5	14	0.13	-	7.4×10^6	-	3.7	15	0.53	-	1.6×10^6	-
200 K	48	a	0.25	-	4.0×10^6	-	53	a	0.88	-	1.1×10^6	-
150 K	1300	a	0.58	-	1.7×10^6	-	1300	a	2.2	-	4.5×10^5	-
120 K	16000	a	2.0	-	5.0×10^5	-	16000	a	8.2	-	1.2×10^5	-
100 K	37000	a	3.1	-	3.2×10^5	-	40000	a	15	-	6.8×10^4	-
80 K	84000	a	5.8	-	1.7×10^5	-	84000	a	27	-	3.6×10^4	-

^a At temperatures of 200 K and lower, the kinetics of the T_{1B} species can not be properly resolved because the depopulation is much faster than the formation, and therefore shows too vague traces in the transients. Furthermore, the formation of the T_{1B} species is hindered below the glass-setting temperature of the solvent mixture (between 150 and 120 K).

TABLE 3: Triplet Lifetimes of ZnP in Toluene/PS (1:1) at Different Temperatures and the Corresponding Rate Constants for Triplet Energy Transfer.

	ZnP-NB			ZnP-NB-H ₂ P			ZnP-BB			ZnP-BB-H ₂ P		
	$\tau_A/\mu\text{s}$	$\tau_B/\mu\text{s}$	$\tau_A/\mu\text{s}$	$\tau_B/\mu\text{s}$	$k_{\text{TETA}}/\text{s}^{-1}$	$k_{\text{TETB}}/\text{s}^{-1}$	$\tau_A/\mu\text{s}$	$\tau_B/\mu\text{s}$	$\tau_A/\mu\text{s}$	$\tau_B/\mu\text{s}$	$k_{\text{TETA}}/\text{s}^{-1}$	$k_{\text{TETB}}/\text{s}^{-1}$
295 K	0.31	9.2	-	5.9	-	6.1×10^4	0.29	9.0	-	8.3	-	9.4×10^3
250 K	4.1	13	0.12	-	8.1×10^6	-	4.2	12	0.42	-	2.1×10^6	-
225 K	6.4	34	0.18	-	5.3×10^6	-	6.5	36	0.87	-	1.0×10^6	-
200 K	400	a	0.35	-	2.9×10^6	-	380	a	1.2	-	8.3×10^5	-
150 K	42000	a	0.95	-	1.1×10^6	-	43000	a	4.1	-	2.4×10^5	-
120 K	56000	a	2.5	-	4.0×10^5	-	54000	a	11	-	9.5×10^4	-
100 K	75000	a	5.1	-	2.0×10^5	-	73000	a	18	-	5.5×10^4	-
80 K	90000	a	8.3	-	1.2×10^5	-	90000	a	30	-	3.4×10^4	-

^a At temperatures of 200 K and lower, the kinetics of the T_{1B} species can not be properly resolved because the depopulation is much faster than the formation, and therefore shows too vague traces in the transients. Furthermore, the formation of the T_{1B} species is hindered below the glass-setting temperature of the solvent mixture (between 200 and 150 K).

TABLE 4: Triplet Lifetimes of ZnP in PS-film at Different Temperatures and the Corresponding Rate Constants for Triplet Energy Transfer.

	ZnP-NB		ZnP-NB-H ₂ P		ZnP-BB		ZnP-BB-H ₂ P	
	τ_A /ms	τ_A / μ s	τ_A / μ s	$k_{\text{TETA}}/\text{s}^{-1}$	τ_A /ms	τ_A / μ s	τ_A / μ s	$k_{\text{TETA}}/\text{s}^{-1}$
295 K	62	4.3	4.3	2.3×10^5	66	5.5	5.5	1.8×10^5
250 K	75	5.2	5.2	1.9×10^5	76	6.0	6.0	1.7×10^5
200 K	81	6.3	6.3	1.6×10^5	81	7.7	7.7	1.3×10^5
150 K	81	7.5	7.5	1.3×10^5	82	9.4	9.4	1.1×10^5
120 K	83	8.9	8.9	1.1×10^5	85	12	12	0.9×10^5
80 K	90	11	11	0.9×10^5	90	16	16	0.6×10^5

Table 5: Activation Energies (ΔG^\ddagger), Reorganization Energies (λ), and Electronic Coupling Elements ($|V|$) for ZnP-NB-H₂P in Different Solvents.

	$\Delta G^\ddagger/\text{kcalmol}^{-1}$			λ/eV			$ V /\text{cm}^{-1}$
	250-120 K ^a	120-80 K	250-120 K ^a	120-80 K	250-120 K ^a	120-80 K	120-80 K
MTHF	1.1	-	0.50	-	0.43		
toluene/MCH	1.6	0.61	0.60	0.41	0.79	0.10	
toluene/PS	1.6	0.66	0.62	0.42	0.74	0.10	
PS-film		0.46 ^b		0.37 ^b		0.033 ^b	

^a 250-150 K for toluene/PS. ^b Parameters determined in the temperature interval RT-80 K. See text for details.

Table 6: Activation Energies (ΔG^\ddagger), Reorganization Energies (λ), and Electronic Coupling Elements ($|V|$) for ZnP-BB-H₂P in Different**Solvents.**

	$\Delta G^\ddagger/\text{kcalmol}^{-1}$			λ/eV			$ V /\text{cm}^{-1}$
	250-120 K ^a	120-80 K	250-120 K ^a	120-80 K	250-120 K ^a	120-80 K	120-80 K
MTHF	1.0	-	0.49	-	0.18		
toluene/MCH	1.6	0.66	0.60	0.42	0.41	0.05	
toluene/PS	1.7	0.58	0.63	0.40	0.39	0.04	
PS-film		0.38 ^b		0.35 ^b		0.027 ^b	

^a 250-150 K for toluene/PS. ^b Parameters determined in the temperature interval RT-80 K. See text for details.

Figure Legends

Figure 1. Structure of the compounds studied in this paper. The zinc and free base porphyrin subunits, ZnP and H_2P , respectively, are covalently linked together by the bridging chromophores, RB , forming the dimers, $ZnP-RB-H_2P$. The bridging chromophores are varied by changing the central unit, R , to be either bicyclo(2.2.2)octane (O), benzene (B) or naphthalene (N). The reference compounds, i.e. zinc or free base porphyrin linked to the bridging chromophores, are denoted $ZnP-RB$ and H_2P-RB , respectively.

Figure 2. Jablonski diagram showing the processes participating in the overall deactivation of ZnP T_{1A} and T_{1B} species in the dimers. The deactivation of the H_2P triplet species has been omitted for clarity. The rate constants are given for low viscosity solvents.

Figure 3. Energy level diagram of the T_{1A} species of the donor (14 000 cm^{-1}), acceptor (12400 cm^{-1})⁴⁵ and the lowest excited triplet states of the bridging chromophores (25 500, 20 000 and 17 500 cm^{-1} for OB , BB , and NB , respectively).

Figure 4. Room temperature ground state absorption spectra of ZnP-NB (·····) and H₂P-NB (—). The Soret band region (λ between 350 and 450 nm) is omitted for clarity.

Figure 5. Room temperature triplet absorption spectra of ZnP-NB (a) and H₂P-NB (b) in MTHF. The numerically resolved spectra of the T_{1A} (o-o-o) and T_{1B} (■-■-■) species are shown and they coincide with the spectra at early and late times, respectively.

Figure 6. Transient absorption decays of ZnP-NB-H₂P at 250 K after excitation at 532 nm. In the short time window (Inset), the decay of the ZnP T_{1A} species is seen in the early part of the transient ($\tau = 95$ ns). In the long time window, three distinct processes are present. The dashed line (- - - -) is the best fit assigned to the overall time evolution of the H₂P absorption (omitting the 95 ns lifetime). The 1.7 μ s risetime seen in the beginning of the transient reflects the transformation process T_{1A}→T_{1B}. The subsequent intersystem crossing T_{1B}→S₀ characterizes the decay at longer times ($\tau = 12.5$ μ s). The corresponding intersystem crossing of ZnP ($\tau = 6.3$ μ s) is also shown (- · - · -). The solid line (—) represents $\Delta A_{\text{tot}}(t)$ in eq. (3), i.e. the total absorption decay of the three triplet species (see text for details).

Figure 7. Temperature dependence of the TET process in the dimers ZnP-BB-H₂P (○) and ZnP-NB-H₂P (■) in MTHF. Solid lines show the best fit to eq. (8).

Figure 8. Temperature dependence of the TET process in the dimers ZnP-BB-H₂P (▼, ■, and ● for toluene/MCH, toluene/PS, and PS-film, respectively) and ZnP-NB-H₂P (▽, □, and ○ for toluene/MCH, toluene/PS, and PS-film, respectively). Solid lines show the best fit to eq. (8).

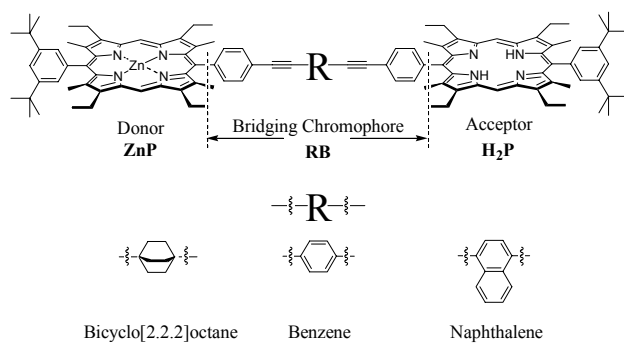


Figure 1, Andréasson et al.

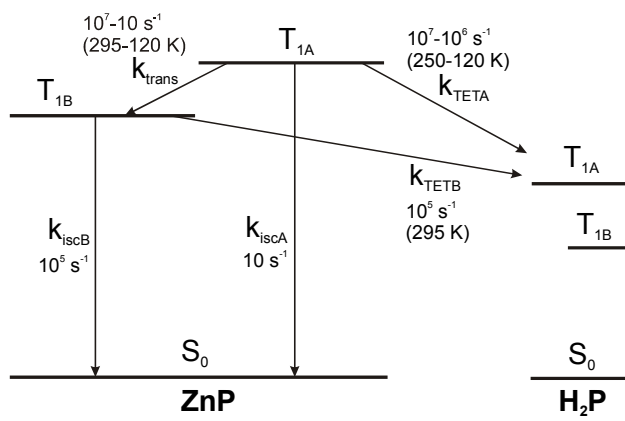


Figure 2, Andréasson et al

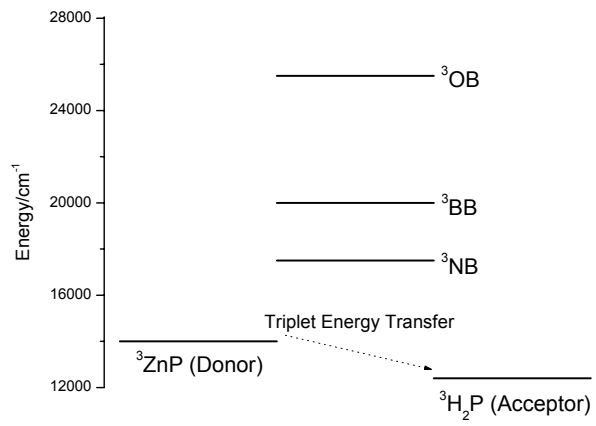


Figure 3, Andréasson et al.

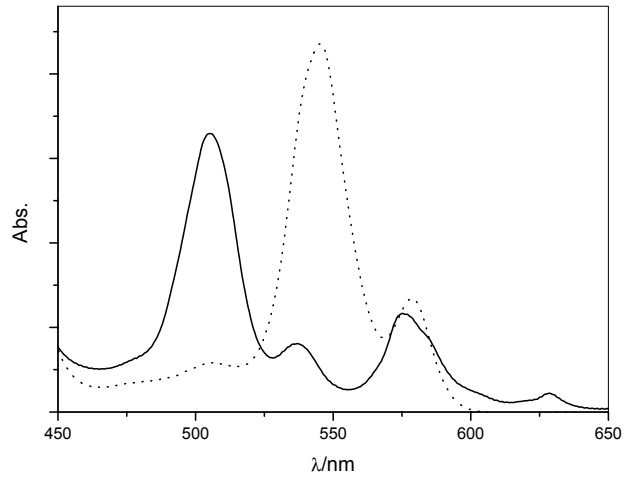


Figure 4, Andréasson et al.

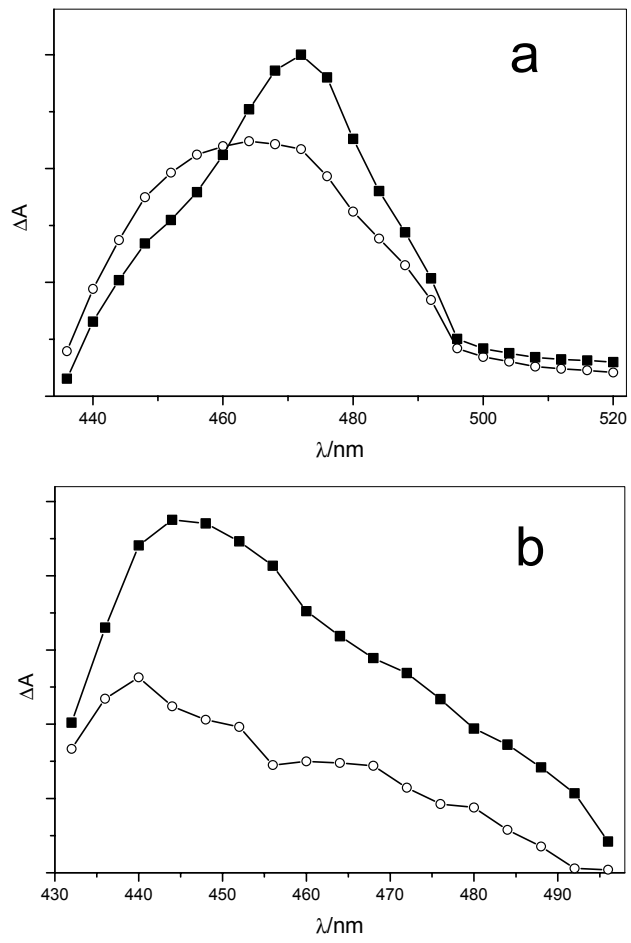


Figure 5, Andréasson et al.

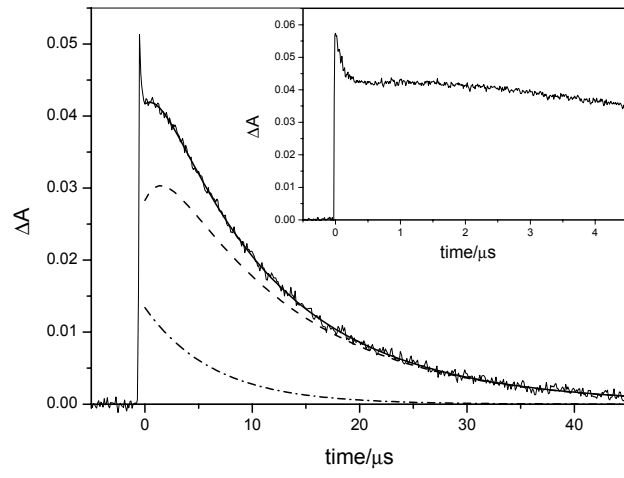


Figure 6, Andréasson et al.

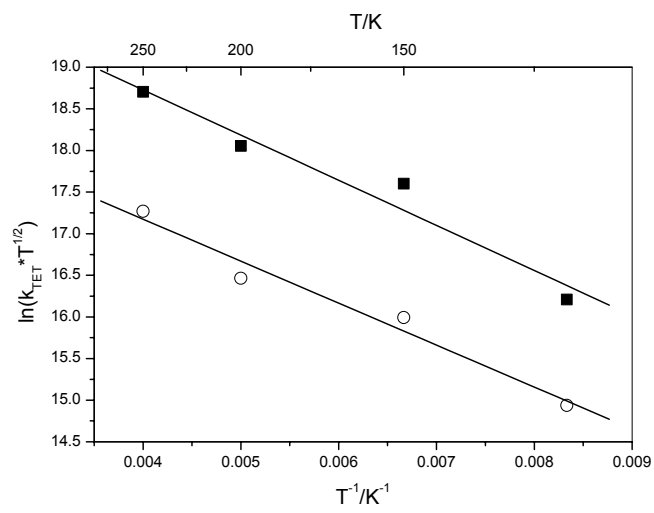


Figure 7, Andréasson et al.

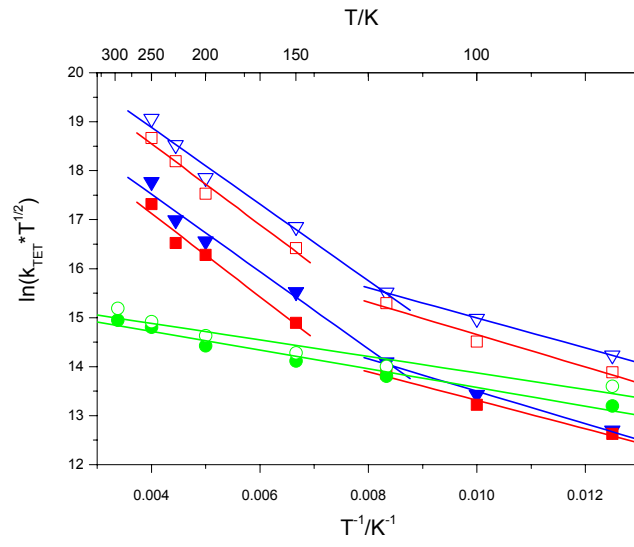


Figure 8, Andréasson et al.